

# Intragastric Distribution and Gastric Emptying Assessed by Three-Dimensional Ultrasonography

ODD HELGE GILJA,\* PAUL R. DETMER,<sup>†</sup> JING MING JONG,<sup>†</sup> DANIEL F. LEOTTA,<sup>§</sup> XIANG-NING LI,<sup>§</sup> KIRK W. BEACH,<sup>†</sup> ROY MARTIN,<sup>§</sup> and D. EUGENE STRANDNESS, Jr.<sup>†</sup>

\*Medical Department A, Haukeland Hospital, University of Bergen, Bergen, Norway; and Departments of <sup>†</sup>Surgery and <sup>§</sup>Anesthesiology and Center for Bioengineering, University of Washington, Seattle, Washington

**Background & Aims:** Three-dimensional (3D) ultrasound imaging of the total stomach volume has not yet been achieved. The aim of this study was to investigate whether a magnetic position sensor system for acquisition of 3D ultrasonograms could be used to determine gastric emptying rates and intragastric distribution.

**Methods:** A system for position and orientation measurement was interfaced to an ultrasound scanner. In vitro accuracy was evaluated by scanning a porcine stomach. Fourteen volunteers, with a median age of 35 years, were scanned fasting and postcibally by two-dimensional (2D) and 3D ultrasound after ingesting a 500-mL soup meal. **Results:** This 3D system yielded a strong correlation ( $r = 0.997$ ) between true and estimated volumes in vitro. The limits of agreement were  $-9.1:70.1$  mL in the volume range 1200–1900 mL. The intersubject variability of the total gastric volumes ranged from 12.5% to 46.0%, less than for antral area variability. The average half-emptying time was  $22.1 \pm 3.8$  minutes. Intragastric distribution of the meal, expressed as proximal distal volume, varied on average from  $3.6 \pm 2.1$  (5 minutes postprandially) to  $2.7 \pm 1.9$  (30 minutes postprandially). **Conclusions:** This 3D ultrasound system using magnetic scanhead tracking showed excellent in vitro accuracy, calculated gastric emptying rates more precisely than by 2D ultrasound, and enabled estimation of intragastric distribution of a soup meal.

Assessment of gastric emptying rates is frequently performed to evaluate patients with motility disorders of the upper gastrointestinal tract. Recently, estimation of intragastric distribution of meals has been added to provide further information on gastric pathophysiology, particularly in patients with functional dyspepsia<sup>1-3</sup> and diabetic visceral neuropathy.<sup>4</sup> The gold standard method to measure these gastric parameters is scintigraphy. However, radionuclide methods expose the subject to radiation and have relatively poor image resolution. Thus, we investigated whether ultrasonography, a radiation-free method, may improve gastric imaging and enhance our understanding of gastric motor function.

Transabdominal two-dimensional (2D) ultrasonography of the stomach has mainly been applied to study antral contractions,<sup>5-7</sup> to calculate standardized areas of the distal stomach,<sup>8-11</sup> to monitor antroduodenal fluid movements,<sup>12-14</sup> and to estimate volumes of the antrum attempting to predict gastric emptying rates.<sup>15-18</sup> The proximal stomach has long been considered inappropriate for ultrasonic imaging because of its position behind the costal margins and the frequent presence of air pockets.<sup>19</sup> In an effort to overcome these limitations, a novel method was recently developed that enabled postprandial scanning of the corpus-fundus while the patients were seated.<sup>20</sup> By using a low-fat soup meal, which served as an excellent contrast agent for the gastrointestinal tract, this method was not restricted to slender individuals and was not dependant on high fat content of the meal. By combining real-time images of the different parts of the stomach, the total stomach volume is now available from transabdominal ultrasonographic examinations.

An early system for acquisition and processing of three-dimensional (3D) ultrasound data was developed in an attempt to enhance the accuracy of volume computation of the distal stomach.<sup>21</sup> Using a motor device, the transducer was tilted through an angle of 90°, capturing sequential 2D frames before the data set was transferred to a graphic workstation for final 3D processing. This 3D ultrasound system was validated both in vitro and in vivo and yielded high accuracy and precision in volume estimation of abdominal organs.<sup>22,23</sup> The system has been used to measure gallbladder volume,<sup>24</sup> to study diseases of the liver,<sup>25</sup> and to evaluate patients with functional dyspepsia.<sup>24,26,27</sup> Despite the significant achievements with respect to accuracy in volume estimation and 3D reconstruction of tissue and organs, this 3D system could

**Abbreviations used in this paper:** 2D, two-dimensional; 3D, three-dimensional; P/D, ratio between the proximal and distal volumes; POM, position and orientation measurement; RMS, root mean square; V<sub>c</sub>, coefficient of variation.

© 1997 by the American Gastroenterological Association  
0016-5085/97/\$3.00

only acquire a 90° fan-like data set from a predetermined, single position of the transducer.

Random or free-hand acquisition of 3D ultrasound data has been achieved using mechanical,<sup>28,29</sup> acoustic,<sup>30–33</sup> or electromagnetic<sup>34,35</sup> devices to locate the exact position and orientation of the transducer in space. Magnetic systems maintain the flexibility and smoothness of free-hand scanning, in contrast to mechanical devices. The acoustic systems are limited by the fact that they do not tolerate physical interruptions of the acoustic wave, e.g., a hand coming in its way, before accuracy is compromised substantially. Accordingly, to enable scanning of a large organ like the fluid-filled stomach, we chose to interface a commercially available magnetometer-based position and orientation measurement (POM) device, which is relatively immune to metallic influence and electronic noise from the scanner. This system for magnetic scan-head tracking has been validated both with respect to its precision in locating specific points in space<sup>35</sup> and to its accuracy in volume estimation.<sup>36,37</sup> In these studies, the sensor system worked well in scanning human organs, and high precision and accuracy were revealed in point location and volume estimation.

The objectives of this study were threefold. First, we aimed to determine the *in vitro* accuracy of the magnetic POM system in volume estimation of a porcine stomach. Second, we wanted to assess whether this system for 3D imaging was applicable for scanning of both the proximal and the distal stomach in humans. Third, if the system worked appropriately for gastric scanning, our purpose was to estimate the intragastric distribution of a meal and the gastric emptying rates.

## Materials and Methods

### Study Design

Healthy volunteers on the staff at the University of Washington were recruited to participate in the trial. Before inclusion into the study, a medical history was obtained and ultrasound examination of the liver, pancreas, and biliary tract was performed to rule out diseases of the upper gastrointestinal system.

Criteria of exclusion from the study were previous surgery in the upper gastrointestinal tract, previous peptic ulcer disease, alcoholism, or use of any medication.

### Subjects

Sixteen healthy individuals, by design all men, entered the trial. The data of 2 subjects could not be analyzed because of derangement of the POM data. The included 14 individuals had a median age of 35 years (range, 26–54 years), weighed  $74 \pm 8$  kg (mean  $\pm$  SD), and their heights were  $178 \pm 6$  cm. Thirteen of the subjects were nonsmokers. To study intraindivi-

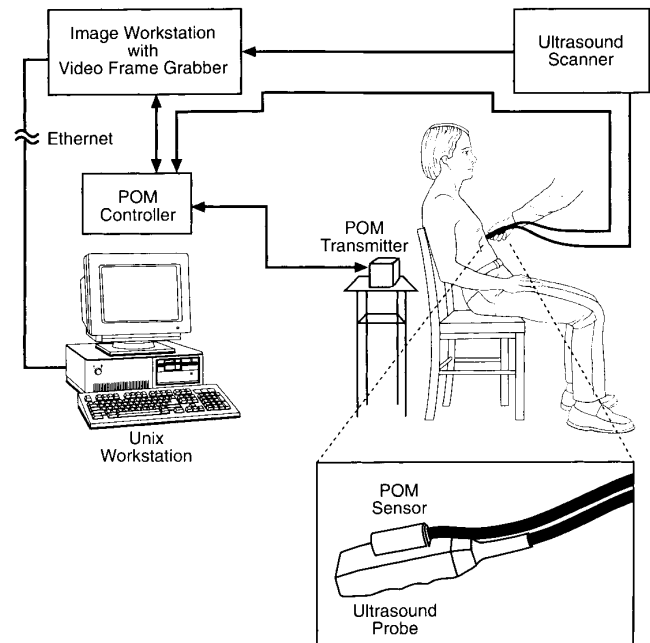


**Figure 1.** Block diagram of the 3D ultrasound system based on magnetic POM. Image and POM data were acquired simultaneously, and the ultrasonograms were digitized from the video output of the scanner by use of a frame grabber board. The POM transmitter was positioned just behind the back of the examined subject and within the performance range of the miniature sensor (60 cm). The data were ultimately transferred via ethernet to a Unix workstation for outlining and volume computation.

vidual variability, 1 healthy man (age, 34 years; weight, 72 kg; height, 178 cm) was examined on 6 consecutive weekdays.

Scanning humans with the POM ultrasound system received human subject approval. The study was conducted in accordance with the revised Declaration of Helsinki. All volunteers gave written, informed consent to participate in the trial.

### Experimental Setup

The 3D imaging system uses a commercial ultrasound scanner (HDI 3000; Advanced Technology Laboratories, Bothell, WA) and a pulsed magnetic field POM system (Miniature Flock of Birds Model 6D FOB; Ascension Technology Corp., Burlington, VT) attached to the ultrasound scanhead. A custom-designed adapter was glued onto the scanhead at a distance of 2 cm from the transducer face, and the miniature sensor was securely mounted into the adapter. The scanner and the Bird system were interfaced to an image acquisition workstation (Image Vue, Nova Microsonics, Mahwah, NJ). The particular scanhead used in this study was a broadband 5–3 MHz hand-held phased array HDI scanhead. Full-frame ultrasound images from the video output of the ultrasound scanner were digitized by a frame grabber board and saved with the POM data to a hard disk. The setup of the system is shown in Figure 1.

The POM system is based on a quasi-DC pulse-flux magnetometer. It consists of an electronic system control unit, a

transmitter module, and a receiving sensor. In-depth description of the POM system and the calibration procedure has been reported previously.<sup>35,38</sup> To calibrate the system, we first determined the precision of the miniature POM system by itself at nine different distances from the transmitter's origin. The miniature sensor alone demonstrated a root mean square (RMS) uncertainty of 2.1 mm over its normal operating range of 500 mm. Second, we measured the precision of the combined POM/ultrasound 3D imaging system, and the RMS uncertainty in point target location was 2.4 mm.

### Test Meal

A liquid meal (500 mL) of commercial meat soup (Toro clear meat soup; Rieber & Søn A/S, Bergen, Norway) containing 1.8 g protein, 0.9 g bovine fat, and 1.1 g carbohydrate (20 kcal) was ingested during a period of 4 minutes. The soup was preheated and then cooled to 37°C, thus improving image quality by reducing the number of air bubbles after ingestion. The pH of the soup varied between 5.4 and 5.7, and the osmolality was 350 mOsm/kg H<sub>2</sub>O. Fat, protein, and carbohydrate were all soluble in water. In addition, the soup contained nonsoluble seasoning (0.4 g/L). In previous studies, this soup meal has induced antral contractions at a frequency of 3/min (fed state) in >85% of both patients with functional dyspepsia and healthy controls.<sup>8,13</sup>

### Experimental Protocol

All participants in the trial ingested the soup meal between 8:25 and 9:52 AM after an overnight fast. The 1 smoker in the study was not allowed to smoke in the morning of the examination. The subjects were scanned while sitting in a chair made of plastic material, leaning slightly backwards at an angle of 120° between the thighs and the spine. The electromagnetic transmitter was positioned close to the back of the volunteer to minimize the distance to the receiver on the scanhead (Figure 2). On average, this distance was approximately 30 cm. Time zero was defined at the start of soup ingestion, and scanning was performed while fasting, and after 5, 10, 15, 20, 25, and 35 minutes. Just before ingestion of the soup, the occurrence of antral contractions was observed for at least 2 minutes to evaluate whether the subject's interdigestive migrating motor complex was in phase III (regular contractions with a frequency of 3/min). If phase III was observed, ingestion of soup was postponed until phase I (quiescence) was observed. All the ultrasound examinations were performed by the same physician (O.H.G.). The test meal may induce dyspepsia in a small proportion of healthy subjects.<sup>9,39</sup> Accordingly, the participants were asked to evaluate their total symptoms after the soup meal on a Likert scale from 0 to 9. Zero denotes no symptoms at all, and 9 denotes excruciating symptoms.

### Data Acquisition

Using the current prototype system, 2 investigators were needed to perform the procedure, 1 to run the image workstation and 1 to scan the volunteer. The ultrasound scan-

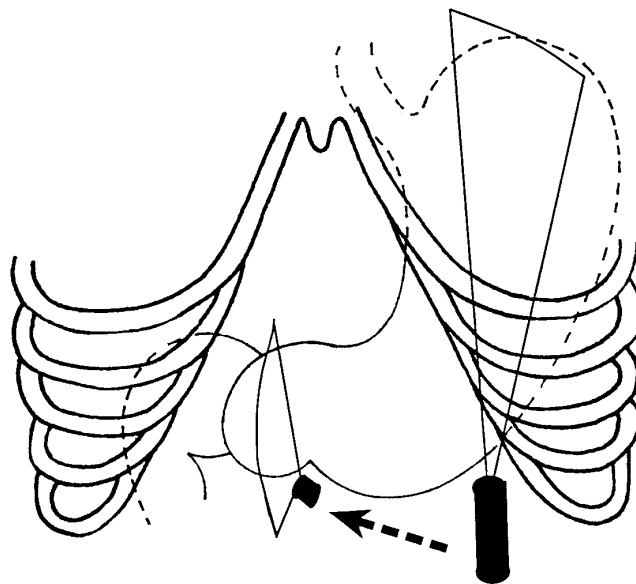


**Figure 2.** Ultrasound scanning of the proximal and distal stomach using magnetic scanhead tracking. Sagittal sections of the stomach were recorded throughout its entire length, starting in the proximal part where the transducer was positioned by the left subcostal margin and tilted cranially to image the most superior part of the stomach. After stepwise scanning of the proximal stomach, the transducer was moved and held to insonify normally to the skin surface. Then the distal stomach was scanned stepwise moving distally to the gastroduodenal junction. Computerized postprocessing of the image, position, and orientation data enabled reconstruction of the total stomach and calculation of volumes, gastric emptying, and intragastric distribution of the meal.

ner was programmed to the same settings before each examination. The depth of scanning was adjusted to fit each individual's habitus, averaging 17.6 cm. The sector angle of the ultrasound image was 80° in all examinations. The sonographer needed approximately 30 seconds per examination just after the meal to determine the optimal starting position for the 3D image scan. Sagittal sections of the stomach were recorded throughout its entire length, starting in the proximal part where the transducer was positioned by the left subcostal margin and tilted cranially to image the most superior part of the stomach. After stepwise scanning of the proximal stomach angling from left to right, the transducer was moved and held to insonify normally to the skin surface. Then the distal stomach was scanned stepwise moving distally to the gastroduodenal junction (Figure 2). The distance between slices of the stomach during acquisition was approximately 0.5 cm. This interslice distance was not kept constant at various degrees of filling because we had no feedback of its magnitude during scanning. That information could only be obtained after computerized postprocessing of the image and position/orientation data.

Gastric contractions can be seen on ultrasonography as pulsatile reductions in antral circumference that occur regularly at a frequency of 3/min postcibally and propagate distally. The delay in time between acquisition of sequential 2D sections

enabled the operators to bypass contractions by receiving visual feedback from the monitor. When gastric contractions were observed, the acquisition was paused until the contraction wave passed the position of the image sector, and then scanning continued "surfing" on the postcontraction wave. In some subjects, particularly in slim individuals, a minor influence of the diaphragm's movement during respiration on the gastric configuration could be observed. If this respiration effect was seen, we aimed to record the largest size of the gastric section, which usually was in passive end expiration. Because each image had to be saved to disk after digitization, the workstation required 5 seconds before the next sonogram could be acquired. On average, the time spent to scan the total gastric volume was 2 minutes, which included the short pauses during contractions. One stepwise scan of the whole stomach usually consisted of 4–5 Mb of data depending on the number of 2D sonograms captured in the 3D scan. The image data and the position and orientation data were transferred to a Unix workstation (DEC Alpha, Digital Equipment Corp., San Jose, CA) for final processing.

In conventional ultrasonography of the distal stomach, a 2D sagittal section is often used, in which the aorta, the superior mesenteric vein, and the gastric antrum are visualized simultaneously,<sup>8,10</sup> permitting repeatable measurements to be taken at the same site. To correlate the volumes of the total and distal stomach obtained by 3D ultrasound to the area of this standardized section, we also acquired 2D images of this section at every time point. The built-in caliper system of the scanner was used to estimate the antral areas by tracing the outer profile of the muscularis propria of the gastric wall.

### Volume Estimation

Computerized volume estimation was performed by using custom software developed within the Application Visualization System software package V5.01 (Advanced Visual Systems Inc., Waltham, MA). This began with interactive manual contour indication on the computer display. The inner echo interface of the gastric mucosa was chosen for manual outlining in all samples. In this study, the two compartments of the stomach were scanned in two separate transducer movements, resulting in overlapping volumes between the proximal and distal stomach often being captured. This problem was overcome by providing the user with a 3D display of the outlines on the workstation, which was updated in real time as the operator traced the sonographic sections. The distal stomach was outlined first, and then the outlines of the proximal stomach were "sewed" onto the distal reconstruction. Overlapping volume regions in the acquisition could thus be separated on the workstation, making volume calculations more straightforward. For the volume estimation of the distal and the proximal stomach, we assume that the gastric compartments do not change volumes significantly during the scanning period of 2 minutes. However, it is likely that small volumes of the soup meal flow from the proximal to the distal compartment in this time span, and also that redistribution may occur. This may lead to inaccuracies in volume estimation. To address

this issue, we calculated an emptying rate of this meal and we determined how often and how much the volume of the proximal stomach increased compared with the previous measurement in the same individual. Thus, an assessment of the antegrade and retrograde flow between the proximal and the distal stomach could be obtained.

Random acquisition of data implies that adjacent sections and contours may intersect, particularly in organs like the stomach where curvatures deep in the abdominal cavity are seen. Thus, a volume computation method for the total stomach volume should take this into account and not simply calculate the volume by summing the volumes between consecutive contours. Surface tiling of the initial 3D point set is very difficult and time consuming and may introduce errors because of the haphazard spacing between the surface points. A volume computation algorithm by Moritz et al.<sup>40</sup> and Martin et al.<sup>41</sup> was reported to provide accurate volume estimation of the cardiac left ventricle after image acquisition by free-hand non-parallel scanning. In this method, the major axis of the ventricle was first derived by linear least square moment analysis among all the outlined points. With the major axis as the center, all the outlined contours were resampled at fixed angles. Then, the resampled points at the same angle from all the contours were sorted to form a link. Subsequently, the total volume was computed by integrating all of the link sections. In the original cardiac algorithm, the main axis needed to be inside all the contours. Applying this algorithm was not a problem for the calculation of the proximal stomach volume if the main axis was derived from the centroids of the contours at both ends. However, because of the curvature of the distal stomach, it was often impossible to find one axis for this part of the gastric cavity. Accordingly, we divided the distal stomach into three parts and assigned one axis for each part. The default ratio for these three parts was 1:2:1 in terms of the number of outlined contours, but the operator could interactively change the joint location of the axis groupings, if necessary. The decision of where to divide the distal stomach into three parts was made during data analysis and did not bear any relationship to anatomic landmarks. The volume of the total stomach was calculated as the sum of the proximal part and three distal parts of the gastric outlines.

The two acquired compartments of the gastric cavity did not necessarily correspond to the actual division between the proximal and the distal stomach. Accordingly, an algorithm was added to the computer program that enabled the line of intersection between the proximal and the distal stomach to be interactively determined. For this study, the intersection line was defined as the 2D section that was located nearest to the angular incisure at the lesser gastric curvature and directed sagittally toward the greater curvature. After this operation, the volumes of the proximal and distal parts of the stomach were computed automatically. A ratio between the proximal (P) volume and the distal (D) volume was calculated at each time point, and this figure (P/D) was used as a measure of intragastric distribution of the meal. The time needed for manual tracing and volume estimation of a scan of the whole stomach was approximately 7 minutes.

### In Vitro Validation

A pig stomach was obtained from a slaughterhouse, thoroughly washed to remove food remnants and debris, and fixed in 20% formalin. The length of the empty stomach measured 26 cm, and the maximum width was 16 cm. A 2.0-mm catheter with Luer lock was surgically attached to the gastroesophageal junction, enabling known volumes of fluid to be infused. Adjacent to the pylorus, a plastic clamp was mounted firmly to seal the gastric cavity, and a syringe (50 mL) was used to infuse tap water. This gastric preparation was positioned between 6 and 19 cm below the surface in a rubber tank of tap water (23°C). Tap water (1200 mL; 23°C) was infused into the gastric lumen, and air pockets trapped in the cavity were carefully removed using the syringe. A 3D scan of the stomach was obtained by stepwise acquisition of 2D images starting at the surface of the water by the proximal end of the stomach. Subsequently, 100 mL of water was added incrementally before the next 3D scan took place. After the last scan at 1900 mL, blue ink was infused to the gastric lumen to confirm that no leakage was occurring.

### Statistical Analysis

The measurements are given as mean values  $\pm$  SD of each parameter, if not stated otherwise. As an initial measure of association between true and estimated volumes, Pearson's correlation coefficient was determined. Furthermore, limits of agreement were estimated as suggested by Bland and Altman.<sup>42</sup> The percent error of the measurements was defined as  $\text{Mean} ([\text{Estimated Volume} - \text{True Volume}] / \text{True Volume}) \times 100\%$ . Linear regression analysis was applied to estimate the gastric emptying rates and half emptying times;  $y$  denotes volume (milliliter) and  $x$  denotes time (minutes). The distribution of data was evaluated by inspecting a probability plot and by using Kolmogorov-Smirnov test with Lilliefors subanalysis. If the data appeared normally distributed, Student's  $t$  test with two-sided probabilities was used to compare differences between the groups. If not normally distributed, a nonparametric test was applied. A  $P$  value  $< 0.05$  was chosen as the level of statistical significance. All calculations and graphic designs were performed using commercially available computer software: Microsoft Excel V5.0 for Windows (Microsoft, Redmond, WA) and Systat V5.0 for Windows (Systat Inc., Evanston, IL).

### Results

The magnetometer-based 3D ultrasound system for acquisition and processing of 3D data proved to be applicable both for in vitro and in vivo imaging of the stomach. The conventional free-hand scanning technique was useful for locating the best suitable acoustic windows for 3D imaging. Neither the scanhead sensor mount plus wiring nor the transmitter mount interfered with the normal scanning procedure.

### In Vitro Validation

To scan a pig stomach with this 3D ultrasound system, 15–19 (median, 17) sonograms were recorded

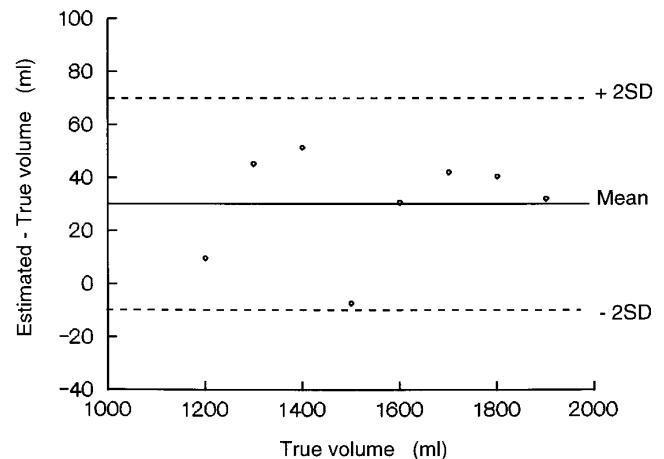


**Figure 3.** Plot displaying the limits of agreement in volume estimation in vitro of the scanning of a porcine stomach by magnetic scanhead tracking. The difference between true volumes (TV), obtained by syringe infusion through a catheter attached to the gastroesophageal junction, and estimated volumes (EV) are depicted on the y-axis. The true volumes are plotted along the x-axis. The 3D ultrasound system overestimated the volume by an average of 30.5 mL over the range of volumes, displaying no proportional error effect.

depending on the volume of the organ. The 3D system yielded an excellent correlation ( $r = 0.997$ ) between true volumes and estimated volumes in a range of 1200–1900 mL. There was no significant correlation between the true and difference between true and estimated volumes ( $r = 0.21$ ;  $P = 0.62$ ). The 3D ultrasound system overestimated the stomach volumes by an average of 30.5 mL over a range of 1200–1900 mL, and the limits of agreement were from  $-9.1$ – $70.1$  mL (Figure 3). The mean error over the volume range was  $2.1\% \pm 1.1\%$ .

### In Vivo Scanning

We acquired a number of 2D scans in the range of  $9 \pm 2$  (fasting) to  $19 \pm 1$  (5 minutes) images to estimate the total stomach volume. The number of sections scanned at 10, 15, 20, 25, and 35 minutes was  $18 \pm 2$ ,  $17 \pm 2$ ,  $16 \pm 2$ ,  $15 \pm 2$ , and  $14 \pm 2$ , respectively. The depths of scanning used to image the stomach were  $12.0 \pm 1.6$  cm for fasting and  $17.9 \pm 0.8$  cm for postprandial acquisitions.

Ultrasonic imaging of 1 healthy volunteer on 6 consecutive days revealed antral area measurement variability postcibally from 3.8% (5 minutes) to 18.2% (35 minutes), given as coefficient of variation ( $V_c$ ). The intraindividual variability of the total gastric volumes ranged from 5.6% (5 minutes) to 34.3% (35 minutes). Full descriptive statistics are listed in Tables 1 and 2. The regression equation describing the total gastric emptying was  $y = 451 - 8.0 \times (\text{SE of estimate, } 16; \text{SE of slope, } 0.7; \text{SE of intercept, } 14)$ , and the corresponding emptying

**Table 1.** Intraindividual Variability in Healthy Subjects of Sagittal Antral Area Measurements in the Aorto-Mesenteric Section Made by 2D Ultrasonography

Antral area	Intraindividual variability (n = 6)				Interindividual variability (n = 14)			
	Mean	SEM	SD	Range	Mean	SEM	SD	Range
Antecibally	5.3	0.5	1.1	3.2	4.3	0.5	1.8	6.0
5 min pc	23.4	0.4	0.9	2.6	20.7	1.4	5.1	17.0
10 min pc	21.1	1.2	3.0	8.1	18.3	1.7	6.3	24.3
15 min pc	19.0	1.3	3.2	8.2	14.0	1.3	4.7	16.5
20 min pc	15.6	1.0	2.5	7.1	11.9	1.1	4.1	15.7
25 min pc	14.4	0.5	1.3	3.4	10.4	1.0	3.8	14.4
35 min pc	11.7	0.9	2.1	5.7	8.3	1.2	4.3	16.0

NOTE. All values are given as centimeters squared. Range is given as the difference between upper and lower limits. pc, postcibally.

rate was 1.8%/min. In the 2-minute scan time period, 3.6% of the soup meal was emptied from the stomach. The proximal, distal, and the total emptying curves are displayed in Figure 4.

The 14 healthy controls demonstrated postprandial antral area measurement variability in the range of 25% (5 minutes) to 52% (35 minutes). Using the antral 2D measurement as a basis for calculation, we found a half emptying time of  $31 \pm 22$  minutes, and  $V_c$  was 70%.

The corresponding variability in total gastric volumes was in the range of 13% (5 minutes) to 46% (35 minutes), showing increasing variability with time. The average total gastric emptying was expressed by  $y = 479 - 11.2 \times$  (SEE, 24; SE of slope, 1.0; SE of intercept, 21). The corresponding values were  $y = 361 - 8.8 \times$  (SEE, 21; SE of slope, 0.9; SE of intercept, 18) for the proximal stomach, and  $y = 115 - 2.2 \times$  (SEE, 6; SE of slope, 0.2; SE of intercept, 5) for the distal stomach. The average half

**Table 2.** Intraindividual and Interindividual Variability of Volume Measurements of the Stomach Based on Image Acquisition by 3D Ultrasonography in Healthy Subjects After Ingestion of a 500-mL Soup Meal

	Intraindividual variability (n = 6)				Interindividual variability (n = 14)			
	Mean	SEM	SD	Range	Mean	SEM	SD	Range
Antecibally								
Total volume	32.9	3.2	8.0	20.0	27.8	5.6	20.9	78.9
5 min pc								
Proximal volume	318.0	8.9	21.8	55.0	327.7	15.6	58.3	257.3
Distal volume	113.7	8.0	19.6	53.4	108.7	10.2	38.1	118.7
Total volume	431.7	9.9	24.2	74.6	436.4	14.6	54.7	171.4
10 min pc								
Proximal volume	252.1	10.9	26.6	76.8	285.0	16.0	60.0	196.1
Distal volume	100.7	6.4	15.6	39.7	86.2	9.0	33.5	109.1
Total volume	352.7	12.8	31.3	94.5	371.2	17.3	64.9	235.4
15 min pc								
Proximal volume	228.5	14.6	35.7	94.4	220.7	20.0	74.7	291.5
Distal volume	90.2	7.5	18.3	44.1	84.6	6.8	25.4	78.4
Total volume	318.7	13.3	32.6	94.1	305.4	17.7	66.4	232.2
20 min pc								
Proximal volume	224.5	19.7	48.2	102.3	172.5	16.1	60.2	188.9
Distal volume	73.4	3.8	9.3	26.2	72.2	6.0	22.5	88.1
Total volume	297.9	20.0	49.0	102.2	244.7	16.2	60.4	164.6
25 min pc								
Proximal volume	183.0	13.7	33.5	95.8	114.6	14.7	55.0	167.3
Distal volume	63.5	4.8	11.7	32.1	52.5	5.4	20.1	69.5
Total volume	246.4	12.4	30.3	80.9	167.1	16.4	61.4	205.3
35 min pc								
Proximal volume	117.4	17.1	42.0	126.8	76.1	12.1	45.1	132.6
Distal volume	59.8	8.3	20.2	55.0	40.9	6.2	23.1	80.5
Total volume	177.2	24.8	60.7	181.8	117.0	14.4	53.9	153.6

NOTE. All volumes are given as milliliters. Range is given as the difference between upper and lower limits. pc, postcibally.

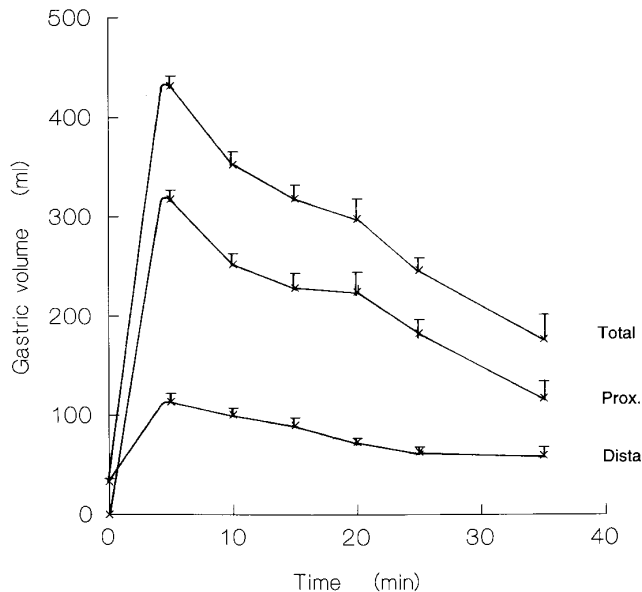


**Figure 4.** Proximal, distal, and total gastric volumes plotted against time to show the day-to-day variability of 1 healthy subject who was scanned on 6 consecutive days. Mean values and SEM are depicted, originating from data acquired by 3D ultrasonography by means of magnetic scanhead tracking.

emptying time of this meal was  $22.1 \pm 3.8$  minutes, based on 3D data, significantly different from half emptying time estimates based on conventional scanning ( $P = 0.026$ ). The proximal, distal, and the total emptying curves are displayed in Figure 5, and the gastric emptying parameters are listed in Table 3.

Intragastric distribution of the meal, expressed as P/D, varied on average from  $3.6 \pm 2.1$  (5 minutes postcibally) to  $2.7 \pm 1.9$  (30 minutes postcibally) (Table 4). Taking all the scans together, the occurrence of retrograde flow was 11/100 (11%) and it was observed in 10 of 20 examinations. The mean volume of retrograde flow was 28.2 mL when measured in intervals of 5 minutes. The only period in which retrograde flow was not observed was the last observation period (30–35 minutes). Wireframe 3D reconstructions of fasting and postprandial stomach volumes are depicted in Figure 6.

None of the healthy subjects experienced any symptoms during or after the meal. No significant correlation was found between age, weight, or height and gastric areas or volumes. When correlating the standard 2D area measurement of the distal stomach with the corresponding 3D distal volume, only the 35-minute estimates were significantly associated ( $r = 0.77$ ;  $P = 0.035$ , Bonferroni). There was no significant correlation between distal area and total gastric volume or between distal volume and total volume at any time point. However, we found an overall correlation between distal area measurements and distal stomach volumes ( $r = 0.67$ ;  $n = 98$ ;  $P <$

0.0005), and between antral area measurements and total stomach volumes ( $r = 0.53$ ;  $n = 84$ ;  $P < 0.005$ ).

## Discussion

The present study shows that a noninvasive and radiation-free method enabled calculation of gastric emptying rates and intragastric distribution of a soup meal in healthy subjects. The use of 3D ultrasonography based on magnetic scanhead tracking permitted images of both the proximal and the distal stomach to be acquired in a translational, stepwise scan. An easy-to-use computer program facilitated outlining of gastric contours and computation of volumes of the gastric compartments. When validated in vitro on a porcine stomach, high accuracy was yielded in volume estimation.

In previous in vitro studies, other investigators reported accuracy of 3D ultrasound systems using mechanical acquisition that was in the same range or lower than in our present study.<sup>40,43,44</sup> Although the present 3D ultrasound system displayed high accuracy in vitro, we cannot immediately extrapolate these results to in vivo conditions. Nevertheless, we have reason to believe that the results obtained in vivo are of acceptable accuracy. First, the mean intercept of the emptying curves of 14 healthy controls was 479.1 mL. Taking into account a mean fasting volume of 27.8 mL, a meal size of 500 mL, and some emptying of the meal during the consumption period,<sup>13</sup> the intercept seems to be at a plausible level.

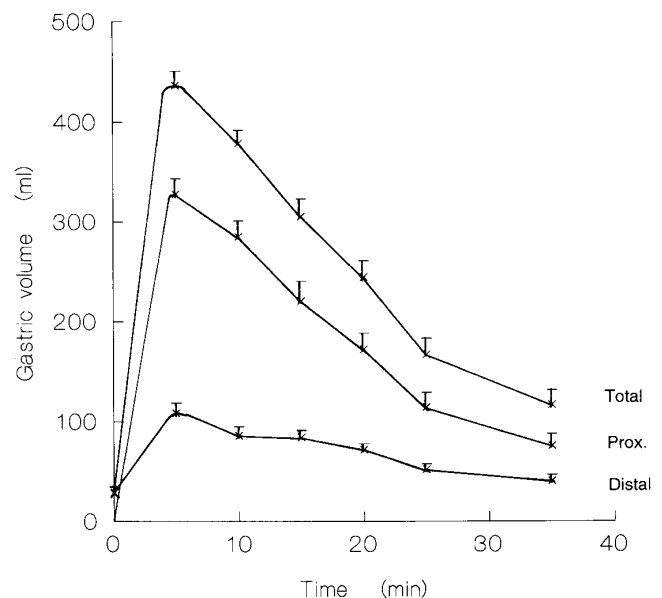


**Figure 5.** Plot of the emptying curves of a soup meal in the proximal, distal, and total gastric compartments of 14 healthy subjects are depicted as mean volumes and SEM. The volumes are obtained from images acquired by 3D ultrasonography based on magnetic scanhead tracking.

**Table 3.** Parameters for Gastric Emptying and Intra-gastric Distribution of a Soup Meal in 1 Healthy Subject Who Was Scanned on 6 Different Days With a 3D Ultrasonographic System

Case	Slope	Intercept	T <sub>1/2</sub>	P/D <sub>5</sub>	P/D <sub>10</sub>	P/D <sub>15</sub>	P/D <sub>20</sub>	P/D <sub>25</sub>	P/D <sub>35</sub>
1	-10.8	468.7	21.7	2.2	2.1	2.5	3.4	2.4	1.4
2	-4.5	414.0	46.0	2.8	2.8	3.6	3.8	3.0	2.0
3	-8.7	462.4	26.6	2.9	2.5	1.7	2.3	2.5	1.8
4	-7.5	454.9	30.3	2.9	3.5	2.4	3.2	5.5	2.6
5	-7.9	439.6	27.8	4.1	2.2	3.6	3.7	2.5	2.2
6	-8.8	464.7	26.4	2.4	2.3	2.0	2.1	2.4	1.8
Mean	-8.0	450.7	29.8	2.9	2.6	2.7	3.1	3.0	2.0
SD	2.1	20.7	8.4	0.6	0.5	0.8	0.7	1.2	0.4
SEM	0.8	8.5	3.4	0.3	0.2	0.3	0.3	0.5	0.2
CV	0.26	0.05	0.28	0.22	0.21	0.31	0.24	0.41	0.21

NOTE. Slope and intercept (milliliters) denotes the time coefficient ( $\alpha$ ) and the constant ( $\beta$ ) derived from linear regression analysis. P/D<sub>5-35</sub> denotes the ratio between proximal and distal gastric volumes at different time points after start of soup ingestion (minutes). T<sub>1/2</sub> denotes half emptying time.

Second, the soup in use was also used in a study where gastric emptying was monitored in healthy controls by radionuclide methods.<sup>45</sup> In this study, a mean half emptying time of  $22.9 \pm 12.1$  minutes was found using scintigraphy, which is close to our finding of  $22.1 \pm 3.8$  minutes. Accordingly, the in vivo data presented in this article appear to be valid and relevant for interpretation of human gastric physiology.

It is well known from scintigraphic studies that gastric emptying data display substantial variability, both intraindividually and interindividually. The variability of the ultrasonic measurements found in our study is comparable to previous radionuclide methodological studies.<sup>46,47</sup> The interindividual variation of antral area measurements using a single 2D sagittal section was greater than the corre-

sponding variation in gastric volumes (Tables 1 and 2). Interestingly, the variability in ultrasound measurements, both within subject and between subjects, increased as emptying proceeded. This observation may be explained by increasing activation of duodeno- and intestino-gastric reflexes throughout the meal-emptying period, inducing relaxation of the proximal stomach to various degrees in different subjects, thus facilitating a wider spectrum of intra-gastric distribution of the meal.<sup>48,49</sup>

The gastric half emptying rates demonstrated that estimates based on 3D data acquisition were significantly smaller and less variable compared with those based on conventional 2D scanning of the antrum. Actually, the variability ( $V_c$ ) of the 2D data was four times higher than the variability of the 3D data, concerning gastric

**Table 4.** Parameters for Gastric Emptying and Intra-gastric Distribution of a Soup Meal in 14 Healthy Subjects Who Were Scanned With a 3D Ultrasonographic System Based on Magnetic Scanhead Tracking

Case	Slope	Intercept	T <sub>1/2</sub>	P/D <sub>5</sub>	P/D <sub>10</sub>	P/D <sub>15</sub>	P/D <sub>20</sub>	P/D <sub>25</sub>	P/D <sub>35</sub>
1	-9.7	481.5	24.8	2.4	2.7	2.6	1.5	1.8	1.2
2	-8.8	480.4	27.3	4.7	3.8	3.7	3.6	3.5	3.0
3	-11.9	440.9	18.5	1.5	2.1	1.1	0.8	0.4	0.2
4	-8.8	466.2	26.5	3.0	2.5	1.7	2.3	2.5	1.8
5	-11.5	487.0	21.2	2.2	2.8	2.0	1.4	1.5	2.2
6	-12.7	445.2	17.5	6.1	2.5	6.9	8.6	7.3	5.9
7	-13.1	441.9	16.9	2.7	4.1	2.6	1.9	0.7	0.0
8	-7.0	376.8	26.9	3.7	1.8	2.1	1.8	1.7	1.5
9	-12.8	453.7	17.7	1.9	1.7	0.8	1.9	1.2	0.4
10	-8.7	440.9	25.3	3.4	3.4	2.2	2.3	1.6	1.1
11	-14.6	601.3	20.6	2.2	2.7	2.6	3.4	5.7	3.9
12	-14.0	595.4	21.3	9.7	9.3	7.4	4.2	2.9	8.9
13	-9.8	492.4	25.1	3.3	7.8	4.3	3.9	4.2	5.3
14	-12.9	504.3	19.5	3.4	2.8	2.9	2.3	2.1	3.7
Mean	-11.2	479.1	22.1	3.6	3.6	3.1	2.8	2.7	2.8
SD	2.3	59.5	3.8	2.1	2.2	2.0	1.9	1.9	2.5
SEM	0.6	15.9	1.0	0.6	0.6	0.5	0.5	0.5	0.7
CV	0.21	0.12	0.17	0.59	0.63	0.64	0.68	0.73	0.91

NOTE. Slope and intercept denotes the time coefficient ( $\alpha$ ) and the constant ( $\beta$ ) derived from linear regression analysis. P/D<sub>5-35</sub> denotes the ratio between proximal and distal gastric volumes at different time points.



half emptying time. Most previous ultrasonic methods to study gastric emptying have used different measures of the antrum to predict total gastric volumes and emptying rates. In this study, there was no significant correlation between antral area and distal or total gastric volume at any time point. In addition, most of the meal was stored in the proximal rather than the distal stomach (Figures 4 and 5); subsequently, the total gastric emptying curve more closely parallels that of the proximal than the distal stomach. Furthermore, phasic contractions change the geometry of the distal stomach to a larger degree than that of the proximal stomach and therefore are more

likely to influence the area over the curve in the distal stomach. One of the advantages of 3D ultrasonography is that no assumptions regarding shape of the stomach have to be made before volume estimation. Accordingly, this 3D ultrasound system may represent a significant step forward with respect to measuring gastric emptying by ultrasound.

Using radionuclide methods, different approaches have been used to divide the stomach into a proximal and a distal region of interest.<sup>50,51</sup> Collins et al.<sup>52,53</sup> reported that the proximal stomach region was defined as the "reservoir" area seen in all subjects for at least the first

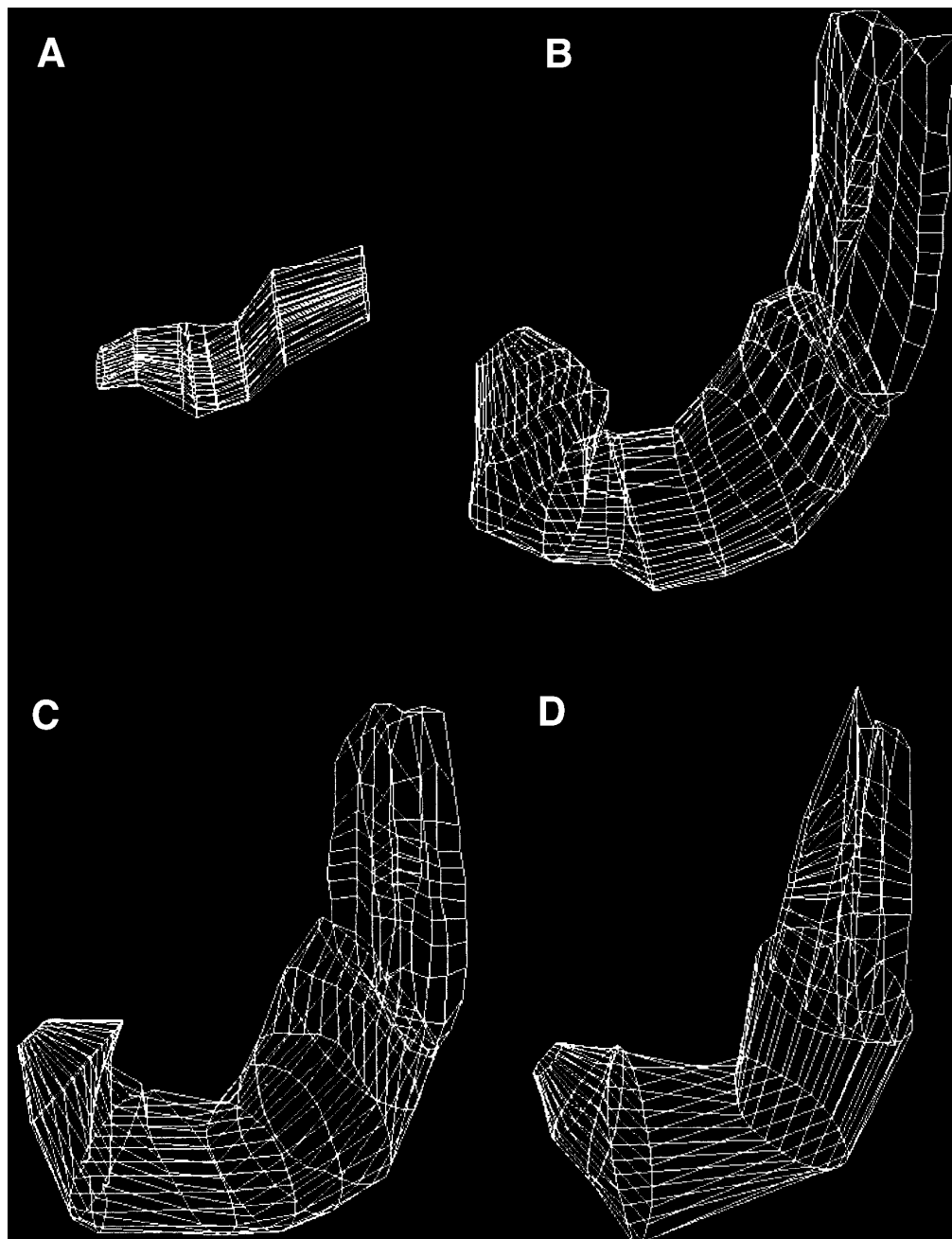


**Figure 6.** 3D wireframes of the stomach of a healthy subject reconstructed from ultrasound images obtained by magnetic scanhead tracking. Panel A is made of antecibal scans, and B, C, and D are outlined from scans 5, 10, and 15 minutes after the soup meal, respectively. Computerized volume reconstruction was performed by using custom software developed within the Application Visualization System software package V5.01 (Advanced Visual Systems Inc., Waltham, MA).

few postcibal frames, and a proximal/distal dividing line was drawn immediately below this region. Another investigator divided the gastric outline at its midpoint by a computer program, with the two regions produced defined as fundus and antrum.<sup>1</sup> In one study, the gastric region of interest was divided into two equal areas, designated the proximal and the distal stomach, by using the cursor facility of the machine to place a line across the stomach so that 50% of the isotope containing pixels was present in each area.<sup>2</sup> Apparently, there seems to be no consensus on how to exactly divide the stomach into a proximal and distal region after scintigraphic scanning. Using ultrasonography, access to anatomic landmarks is provided by the images, giving the operator the choice to base the decision on either anatomic or functional considerations. Contrary to radionuclide methods, ultrasonography offers high image resolution and frame rates that enable exact delineation of the stomach wall without inducing repositioning errors during the examination. In our study, we chose the angular incisure located at the minor curvature as guidance for the division between the distal and the proximal stomach. This anatomic landmark is easily visualized by ultrasonography. In our opinion, the use of ultrasonography to determine the division line is more precise than the radionuclide methods outlined above.

Intragastric distribution is a parameter that has mainly been adopted for studies of patients with functional dyspepsia. Several investigators have indicated that these patients show abnormal intragastric distribution of the meal, as evaluated by scintigraphy.<sup>1-3</sup> In our study on healthy subjects, we observed a relatively high P/D initially, declining as the meal emptied. Interestingly, we found that retrograde flow from the distal to the proximal stomach occurred in 11% of measurement periods, and it was observed in half of the examinations. It is worth noting that the high intersubject variability in the P/D data makes it questionable if intragastric distribution is a useful parameter in diagnosis and work-up of patients. Nevertheless, further development of hardware and software for 3D ultrasonic image acquisition are in progress and may improve spatial and temporal resolution of this technique significantly, thus enabling a more precise and consistent division of the gastric compartments.

This study was subject to the same limitations of ultrasound scanning that are generally observed in other studies. The method is fairly operator-dependent and may be influenced by the presence of air pockets within the fundus, which dramatically reduces image quality. This problem was addressed in previous studies using the same soup meal, both in healthy controls<sup>20</sup> and in patients with functional dyspepsia.<sup>39</sup> These studies showed that

air in the gastric fundus was not a critical factor for ultrasonic imaging using this meal, and no subjects had to be excluded for this reason. Similarly, in the present study, gas pockets in the fundus did not impair visualization of the proximal stomach to such an extent that data could not be analyzed. We believe that the method of heating the meal to the boiling point and then cooling it to body temperature generates less air bubbles in the stomach than a meal at room temperature that is ingested. Furthermore, the seated position with the individuals leaning slightly backward was probably optimal with respect to distribution of air within the stomach. If any of the volunteers experienced an urge to burp during or just after the ingestion of the soup, they were encouraged to do so.

Compared with ordinary ultrasound equipment, this 3D system based on magnetic scanhead tracking, although less than for comparable magnetic systems, is susceptible to metallic influence and to interference from external magnetic fields. Therefore, it is of major importance that the laboratory environment is evaluated carefully to avoid spatial distortion of data. The distance from the scanner itself to the sensor on the scanhead should preferably be at least 60 cm, and the bed or chair must be made of material that does not influence magnetic fields. Despite our efforts to remove watches, belts, coins, etc. from both the operators and the participants, two of the data sets were distorted, probably because of magnetic interference from nearby experiments in the laboratory.

An acquisition time of 2 minutes was used in this study because the image workstation design required that it store each captured image to hard disk before the next acquisition. By using image acquisition systems that enable storing of data in random access memory, the acquisition of a total gastric volume could easily be reduced to less than 30 seconds. The long scanning time experienced in this study may have caused a small intragastric volume to empty through the pylorus or possibly to change compartments during the scanning procedure. Conversely, the slow pace of data capture gave the operator time to carefully select images of high quality and to avoid capturing gastric contractions in the data set, thus minimizing potential errors in volume calculation.

This novel ultrasonographic method to scan the human stomach may be used to evaluate patients with functional dyspepsia, diabetes mellitus, and other conditions in which gastroparesis and maldistribution is a prominent feature. However, before further application of this method in clinical settings, validation against the gold standard at present, scintigraphy, would be reasonable. Furthermore, caution needs to be exercised before our

results can be extrapolated to gastric emptying of solids. In conclusion, we found that the present 3D ultrasonographic method based on magnetic scanhead tracking demonstrated high accuracy in vitro. The 3D system computed gastric emptying parameters more precisely than conventional 2D ultrasonography in healthy individuals. Furthermore, intragastric distribution of a meal could be determined based on detailed segmentation of gastric compartments.

## References

1. Scott AM, Kellow JE, Shuter B, Cowan H, Corbett AM, Riley JW, Lunzer MR, Eckstein RP, Hoschl R, Lam SK, Jones MP. Intragastric distribution and gastric emptying of solids and liquids in functional dyspepsia. Lack of influence of symptom subgroups and *H. pylori*-associated gastritis. *Dig Dis Sci* 1993;38:2247-2254.
2. Troncon LEA, Bennett RJ, Ahluwalia NK, Thompson DG. Abnormal intragastric distribution of food during gastric emptying in functional dyspepsia patients. *Gut* 1994;35:327-332.
3. Mangnall YF, Houghton LA, Johnson AG, Read NW. Abnormal distribution of a fatty liquid test meal within the stomach of patients with non-ulcer dyspepsia. *Eur J Gastroenterol Hepatol* 1994;6:323-327.
4. Jones KL, Horowitz M, Wishart MJ, Maddox AF, Harding PE, Chatterton BE. Relationships between gastric emptying, intragastric meal distribution and blood glucose concentrations in diabetes mellitus. *J Nucl Med* 1995;36:2220-2228.
5. Holt S, McDicken WN, Anderson T, Stewart IC, Heading RC. Dynamic imaging of the stomach by real-time ultrasound—a method for the study of gastric motility. *Gut* 1980;21:597-601.
6. Hausken T, Odegaard S, Berstad A. Antroduodenal motility studied by real-time ultrasonography. Effect of enprostil. *Gastroenterology* 1991;100:59-63.
7. Vogelberg KH, Rathmann W, Helbig G. Sonographic examination of gastric motility in diabetics with autonomic neuropathy. *Diabetes Res* 1987;5:175-179.
8. Hausken T, Berstad A. Wide gastric antrum in patients with non-ulcer dyspepsia. Effect of cisapride. *Scand J Gastroenterol* 1992;27:427-432.
9. Hausken T, Svebak S, Wilhelmsen I, Tangen Haug T, Olafsen K, Pettersson E, Hveem K, Berstad A. Low vagal tone and antral dysmotility in patients with functional dyspepsia. *Psychosom Med* 1993;55:12-22.
10. Durlars D, Schilling D, Riemann JF. The feasibility of ultrasonography for the evaluation of stomach motility disorders. *Dtsch Med Wochenschr* 1994;119:575-580.
11. Duan LP, Zheng ZT, Li YN. A study of gastric emptying in non-ulcer dyspepsia using a new ultrasonographic method. *Scand J Gastroenterol* 1993;28:355-360.
12. King PM, Adam RD, Pryde A, McDicken WN, Heading RC. Relationships of human antroduodenal motility and transpyloric fluid movement: non-invasive observations with real-time ultrasound. *Gut* 1984;25:1384-1391.
13. Hausken T, Odegaard S, Matre K, Berstad A. Antroduodenal motility and movements of luminal contents studied by duplex sonography. *Gastroenterology* 1992;102:1583-1590.
14. Brown BP, Schulze Delrieu K, Schrier JE, Abu Yousef MM. The configuration of the human gastroduodenal junction in the separate emptying of liquids and solids. *Gastroenterology* 1993;105:433-440.
15. Bateman DN, Whittingham TA. Measurement of gastric emptying by real-time ultrasound. *Gut* 1982;23:524-527.
16. Bolondi L, Bortolotti M, Santi V, Calletti T, Gaiani S, Labo G. Measurement of gastric emptying time by real-time ultrasonography. *Gastroenterology* 1985;89:752-759.
17. Ricci R, Bontempo I, Corazzari E, La Bella A, Torsoli A. Real time ultrasonography of the gastric antrum. *Gut* 1993;34:173-176.
18. Holt S, Cervantes J, Wilkinson AA, Wallace JH. Measurement of gastric emptying rate in humans by real-time ultrasound. *Gastroenterology* 1986;90:918-923.
19. Tomooka Y, Onitsuka H, Goya T, Koga T, Uchida S, Russell WJ, Torisu M. Ultrasonography of benign gastric ulcers. Characteristic features and sequential follow-ups. *J Ultrasound Med* 1989;8:513-517.
20. Gilja OH, Hausken T, Odegaard S, Berstad A. Monitoring postprandial size of the proximal stomach by ultrasonography. *J Ultrasound Med* 1995;14:81-89.
21. Thune N, Hausken T, Gilja OH, Matre K. A practical method for estimating enclosed volumes using 3D ultrasound. *Eur J Ultrasound* 1996;3:83-92.
22. Gilja OH, Thune N, Matre K, Hausken T, Odegaard S, Berstad A. In vitro evaluation of three-dimensional ultrasonography in volume estimation of abdominal organs. *Ultrasound Med Biol* 1994;20:157-165.
23. Gilja OH, Smievoll AI, Thune N, Matre K, Hausken T, Odegaard S, Berstad A. In vivo comparison of 3D ultrasonography and magnetic resonance imaging in volume estimation of human kidneys. *Ultrasound Med Biol* 1995;21:25-32.
24. Hausken T, Thune N, Matre K, Gilja OH, Odegaard S, Berstad A. Volume estimation of the gastric antrum and the gallbladder in patients with non-ulcer dyspepsia and erosive prepyloric changes, using three-dimensional ultrasonography. *Neurogastroenterol Motil* 1994;6:263-270.
25. Hokland J, Hausken T. An interactive volume rendering method applied to ultrasonography of abdominal structures. *IEEE Ultrason Symp Proc* 1994;3:1567-1571.
26. Gilja OH, Hausken T, Berstad A. Three-dimensional ultrasonography of the gastric antrum in patients with functional dyspepsia (abstr). *Gastroenterology* 1995;108:A605.
27. Berstad A, Hausken T, Gilja OH, Thune N, Matre K, Odegaard S. Volume measurement of gastric antrum by 3-D ultrasonography and flow measurements through the pylorus by duplex technique. *Dig Dis Sci* 1994;39:97-100.
28. Dekker DL, Piziali RL, Dong EJ. A system for ultrasonically imaging the human heart in three dimensions. *Comput Biomed Res* 1974;7:544-553.
29. Nikraves PE, Skorton DJ, Chandran KB, Attarwala YM, Pandian N, Kerber RE. Computerized three-dimensional finite element reconstruction of the left ventricle from cross-sectional echocardiograms. *Ultrason Imaging* 1984;6:48-59.
30. Moritz WE, Shreve PL, Mace LE. Analysis of an ultrasonic spatial locating system. *IEEE Trans Instrum Meas* 1976;25:43-50.
31. Brinkley JF, Muramatsu SK, McCallum WD, Popp RL. In vitro evaluation of an ultrasonic three-dimensional imaging and volume system. *Ultrason Imaging* 1982;4:126-139.
32. Handschumacher MD, Lethor JP, Siu SC, Mele D, Rivera JM, Picard MH, Weyman AE, Levine RA. A new integrated system for three-dimensional echocardiographic reconstruction: development and validation for ventricular volume with application in human subjects. *J Am Coll Cardiol* 1993;21:743-753.
33. Levine RA, Handschumacher MD, Sanfilippo AJ, Hagege AA, Harrihan P, Marshall JE, Weyman AE. Three-dimensional echocardiographic reconstruction of the mitral valve, with implications for the diagnosis of mitral valve prolapse. *Circulation* 1989;80:589-598.
34. Kelly IM, Gardener JE, Brett AD, Richards R, Lees WR. Three-dimensional US of the fetus. Work in progress. *Radiology* 1994;192:253-259.
35. Detmer PR, Bashein G, Hodges TC, Beach KW, Filer EP, Burns

- DH, Strandness DE, Jr. 3D ultrasonic image feature localization based on magnetic scanhead tracking: in vitro calibration and validation. *Ultrasound Med Biol* 1995;20:923-936.
36. Hodges TC, Detmer PR, Burns DH, Beach KW, Strandness DE, Jr. Ultrasonic three-dimensional reconstruction: in vitro and in vivo volume and area measurement. *Ultrasound Med Biol* 1994;20:719-729.
  37. Gilja OH, Hausken T, Olafsson S, Matre K, Odegaard S. In vitro evaluation of three-dimensional ultrasonography based on magnetic scanhead tracking (abstr). *Ultraschall Med* 1995;16:24.
  38. Leotta DF, Detmer PR, Gilja OH, Jong JM, Martin RW, Primozich JF, Beach KW, Strandness DE, Jr. Three-dimensional ultrasound imaging using multiple magnetic tracking systems and miniature magnetic sensors. *Proc IEEE Int Ultrasonics Symp* 1995, Seattle, WA: 1415-1418.
  39. Gilja OH, Hausken T, Wilhelmsen I, Berstad A. Impaired accommodation of the proximal stomach to a soup meal in functional dyspepsia. *Dig Dis Sci* 1996;41:689-696.
  40. Moritz WE, Pearlman AS, McCabe DH, Medema DK, Ainsworth ME, Boles MS. An ultrasonic technique for imaging the ventricle in three dimensions and calculating its volume. *IEEE Trans Biomed Eng* 1983;30:482-491.
  41. Martin RW, Bashein G, Detmer PR, Moritz WE. Ventricular volume measurement from a multiplanar transesophageal ultrasonic imaging system: an in vitro study. *IEEE Trans Biomed Eng* 1990;37:442-449.
  42. Bland JM, Altman DG. Statistical methods for assessing agreement between two methods of clinical measurements. *Lancet* 1986;1:307-310.
  43. Ariet M, Geiser EA, Lupkiewicz SM, Conetta DA, Conti CR. Evaluation of a three-dimensional reconstruction to compute left ventricular volume and mass. *Am J Cardiol* 1984;54:415-420.
  44. Basset O, Gimenez G, Mestas JL, Cathignol D, Devonec M. Volume measurement by ultrasonic transverse or sagittal cross-sectional scanning. *Ultrasound Med Biol* 1991;17:291-296.
  45. Hveem K, Jones K, Chatterton BE, Horowitz M. Scintigraphic and ultrasonographic measurement of the antral area—relationship to appetite. *Gut* 1996;38:816-821.
  46. Lawaetz O, Dige Petersen H. Gastric emptying of liquid meals. A study in 88 normal persons. *Ann Chir Gynaecol* 1989;78:267-276.
  47. Brophy CM, Moore JG, Christian PE, Egger MJ, Taylor AT. Variability of gastric emptying measurements in man employing standardized radiolabeled meals. *Dig Dis Sci* 1986;31:799-806.
  48. Azpiroz F, Malagelada JR. Isobaric intestinal distension in humans: sensorial relay and reflex gastric relaxation. *Am J Physiol* 1990;258:G202-G207.
  49. De Ponti F, Azpiroz F, Malagelada JR. Reflex gastric relaxation in response to distention of the duodenum. *Am J Physiol* 1987;252:G595-G601.
  50. Barker MC, Cobden I, Axon AT. Proximal stomach and antrum in stomach emptying. *Gut* 1979;20:309-311.
  51. Lawaetz O, Aritas Y, Brown NJ, Ralphs DN, Sjontoft E. Distribution of a liquid meal within the stomach and gastric emptying after vagotomy and drainage operations. *Gut* 1982;23:683-691.
  52. Collins PJ, Horowitz M, Chatterton BE. Proximal, distal and total stomach emptying of a digestible solid meal in normal subjects. *Br J Radiol* 1988;61:12-18.
  53. Collins PJ, Houghton LA, Read NW, Horowitz M, Chatterton BE, Hedde R, Dent J. Role of the proximal and distal stomach in mixed solid and liquid meal emptying. *Gut* 1991;32:615-619.

---

Received September 4, 1996. Accepted March 13, 1997.

Address requests for reprints to: Odd Helge Gilja, M.D., Ph.D., Medical Department A, Haukeland Hospital, University of Bergen, N-5021 Bergen, Norway. e-mail: Odd.Gilja@meda.uib.no; fax: (47) 55-972950.

Supported by The Norwegian Research Council, Odd Fellow Medical Research Foundation (Norway), Astri and Edvard Riisøen's Legacy, and Nycomed Pharma (Norway) and a grant from the University of Washington Royalty Research Fund. The 3D acquisition system was provided by National Institutes of Health grants HL41464 and R43RR07741 and the processing and display equipment by National Institutes of Health HL42270.

The authors thank Prof. Svein Ødegaard, who facilitated the collaboration between the University of Washington and the University of Bergen, and Advanced Technology Laboratory (Bothell, WA) for providing the ultrasound system.